

Modelling the Spatially Varying Non-Linear Effects of Heat Exposure

Xinyi Chen¹, Marta Blangiardo¹, Connor Gascoigne¹, and Garyfallos
Konstantinoudis^{2,*}

¹MRC Centre for Environment and Health, School of Public Health, Imperial
College London, London, UK

²Grantham Institute for Climate Change and the Environment, Imperial
College London, London, UK

* Corresponding author. Garyfallos Konstantinoudis, Grantham Institute for
Climate Change and the Environment, Imperial College London, London, UK.
g.konstantinoudis@imperial.ac.uk

Abstract

Exposure to high ambient temperatures is a significant driver of preventable mortality, with non-linear health effects and elevated risks in specific regions. To capture this complexity and account for spatial dependencies across small areas, we propose a Bayesian framework that integrates non-linear functions with the Besag, York, and Mollié (BYM2) model. Applying this framework to all-cause mortality data in Switzerland, we quantified spatial inequalities in heat-related mortality. We retrieved daily all-cause mortality at small areas (2,145 municipalities) for people older than 65 years from the Swiss Federal Office of Public Health and daily mean temperature at $1\text{km} \times 1\text{km}$ grid from the Swiss Federal Office of Meteorology. By fully propagating uncertainties, we derived key epidemiological metrics, including heat-related excess mortality and minimum mortality temperature (MMT). Heat-related excess mortality rates were higher in northern Switzerland, while lower MMTs were observed in mountainous regions. Further, we explored the role of the proportion of individuals older than 85 years, green space, average temperature, deprivation, urbanicity, and language regions in explaining these discrepancies. We found that spatial disparities in heat-related excess mortality were primarily driven by population age distribution, green space, and vulnerabilities associated with elevated temperature exposure.

Keywords: epidemiological metrics, heat exposure, mortality, natural cubic splines, spatial model

1 Introduction

Exposure to high ambient temperatures can result in increased illness and mortality (Ebi et al., 2021; Vicedo-Cabrera et al., 2023). The relationship between heat exposure and health is non-linear and typically follows a J-shaped curve (Gasparrini et al., 2015; Gasparrini and Armstrong, 2010; Gasparrini, 2022; Èrica Martínez-Solanas et al., 2021), indicating that whilst mild-to-moderate heat may have limited impact, extreme heat can lead to a sharp rise in adverse health effects. The short-term effect of heat exposure on mortality is commonly assessed using a time series approach which allows for non-linearity in the relationship, commonly captured using splines (Gasparrini et al., 2015; Gasparrini and Armstrong, 2010; Gasparrini, 2022; Èrica Martínez-Solanas et al., 2021), and accounts for effect modifiers through stratification or meta-analyses (Ballester et al., 2023; Vicedo-Cabrera et al., 2023; Gasparrini et al., 2015; Masselot et al., 2023; Gasparrini et al., 2010, 2012; Gasparrini and Armstrong, 2010).

Previous studies have reported individual and spatial vulnerabilities due to the effect of heat. Studies have shown how older populations and individuals with chronic conditions, such as cardiorespiratory diseases and diabetes, are more vulnerable to heat exposure due to lower efficiency in body temperature adaptation (Arsad et al., 2022; Ballester et al., 2023). The relationship has also been found to vary by sex, which can be explained by variation in physical, socio-cultural or lifestyle factors (Ballester et al., 2023). Studies focusing on quantifying the spatial vulnerabilities of heat exposure have reported that the effect of heat can be modified by local characteristics, such as deprivation, access to medical healthcare services, green space and urbanicity (Arsad et al., 2022; Gasparrini et al., 2022). Most of these studies did not account for the spatial correlation of temperature effects at a small-area level, likely resulting in imprecise point estimates.

Whilst some studies have accounted for the spatial dependence of the temperature effect using a Bayesian spatio-temporal models, most have considered a linear threshold model, which cannot fully accommodate a non-linear relationship (Konstantinoudis et al., 2022; Bennett et al., 2014). One study focusing on the city of Barcelona modelled the non-linear effect of temperature on mortality, implementing spatially-varying (at 73 neighbourhoods) coefficients of the spline basis function (Quijal-Zamorano et al., 2024; Rue et al., 2009). However, the conditional autoregressive prior they proposed (Leroux et al., 2000) is not scaled, hampering the interpretation of the hyperpriors in other settings. (Riebler et al., 2016). In addition, they did not account for population size or allowed for residual spatial variation through random effects, choices which likely confound the estimated relationship. Finally, they did not provide ways of examining potential spatial

effect modifiers to explain the observed spatial variation in the effects of temperature.

In this project, we propose a flexible model within a Bayesian framework, which is able to account for the spatial variation of the temperature effects, as well as for the spatio-temporal residual confounding. Whilst this is framed in a similar perspective to Quijal-Zamorano et al. (2024) using the INLA algorithm (Rue et al., 2009), we extend and develop the results in three ways. Firstly, we scale the problem from a city-based analysis to a nationwide scenario, considering 2,145 municipalities within 26 cantons across the whole country of Switzerland from 2011 to 2022. Secondly, we address the scaling issue of the conditional autoregressive prior by incorporating Gaussian priors which ensure scalability and identifiability in conjunction with hyperpriors that penalise model complexity ensuring the inference is not overly reliant on the prior specification. Thirdly and finally, we derive a set of epidemiological metrics relevant for results dissemination which we then use in a secondary analysis to quantify the effects of observed and unobserved environmental factors in the estimated spatial vulnerabilities to the effects of heat.

The remainder of the paper is structured as follows: In Section 2, we describe the dataset used for the analyses. In Section 3, we introduce the statistical approach to account for the spatial variation and spatial dependence of the non-linear heat effects across the municipalities, the calculation methods of epidemiological metrics, and the model to conduct the secondary spatial effect modifier analysis. In Section 4, we introduce different complementary epidemiological metrics derived from our model framework and the results of the secondary spatial effect modifier analysis, which can be used to obtain a comprehensive picture of the effects of heat on all-cause mortality in Switzerland. Finally we discuss the results and make concluding remarks in Section 5.

2 Data description

We retrieved the daily all-cause mortality data and population data between 1st of June and 31st of August each year covering 2011-2022 in 2,145 municipalities within 26 cantons in Switzerland from the Swiss Federal Office of Public Health (Federal Statistical Office, 2024). A map of Switzerland and its cantons is shown in Supplementary Figure 1. We focused on the summer months due to our interest in heat-related exposures, but the algorithm can be extended to capture the cold-related effects and incorporate longer lags (Gasparrini et al., 2010, 2015). As only yearly population is available (on the 31st of December for each year), we used linear interpolation by municipality to estimate the daily summer population from 2011 to 2022. Based on the results of Ballester et al. (2023), we restricted our analysis to individuals aged over 65 years, as they experience

higher vulnerability to heat exposure.

During the same time period, we retrieved the daily mean temperature at $1\text{km}\times 1\text{km}$ grid from the Federal Office for Meteorology and Climatology (MeteoSwiss, 2020). We obtained average daily municipality temperature by taking a population-weighted average of the grids that cover each municipality, as described previously (de Schrijver et al., 2021). We accounted for up to a 3-day lagged exposure by taking the mean of the temperature exposures across lags 0-3 (Baccini et al., 2008; Gasparrini et al., 2010; Bennett et al., 2014). We adjusted the analysis for national holidays (Nager.Date, 2024), day of week, year (to represent long-term trends) and day of year (to represent seasonality).

We considered the following spatial effect modifiers: language region (Federal Statistical Office, 2010), urbanicity (eurostat, 2011), deprivation (Panczak et al., 2012), green space (Swiss Data Cube, 2020), average temperature across the period, and proportion of people older than 85 years old. We classified the language region into three groups: German, French, and Italian, reflecting different lifestyle factors across Switzerland. For urbanicity, we defined three categories: rural areas (representing thinly-populated rural regions), semi-urban areas (consisting of towns and suburbs or small urban area), and urban areas (including cities and large urban regions). This captures different temperature exposures across the different urban settings. To account for deprivation, we categorized the continuous socioeconomic position (SEP) data, which is a Swiss-based index strongly associated with household income (Panczak et al., 2012), into three groups: low SEP (1st quartile), baseline SEP (2nd and 3rd quartile), and high SEP (4th quartile). As a measure of green space, we used the Normalized Difference Vegetation Index (NDVI) available for 2011 and 2013-2018 (Swiss Data Cube, 2020). We averaged the available NDVI data to represent the green space coverage from 2011 to 2022. To account for potential adaptation mechanisms to higher temperatures, we calculated the mean temperatures across municipalities during the study period. Finally, using the population data, we defined the proportion of population older than 85 years old, as they are expected to be more vulnerable to heat exposure.

3 Methods

Our approach consists of three steps: (i) we model the effects of temperature on summer mortality in Switzerland; (ii) we estimate a range of epidemiological metrics to fully explore the heat-mortality relationship; (iii) we disentangle the spatial vulnerabilities of heat exposure on all-cause mortality by modelling the relationship between one of the epidemiological metrics, heat-related excess mortality rate, and the spatial effect modifiers

(language region, urbanicity, deprivation, green space, average temperature, and proportion of people over the age of 85). The statistical analyses are performed in R 4.4.1 (R Core Team, 2024).

3.1 Statistical approach

Let Y_{dtm} be the number of deaths for all causes, for the d -th day in t -th year, and m -th municipality. As we restrict our analysis to the summer months (June, July, August), we use $d = 1, \dots, 92$ for the day index, $t = 1, \dots, 12$ for the year (2011 to 2022), and $m = 1, \dots, 2145$ for the municipalities.

In the first step, we model the relationship between all-cause mortality and temperature using a Poisson likelihood with a log-link function,

$$Y_{dtm} \sim \text{Poisson}(E[Y_{dtm}])$$

$$\log(E[Y_{dtm}]) = \log(P_{dtm}) + \beta_0 + \mathbf{X}_{dtm} \cdot \boldsymbol{\beta}_m + \mathbf{Z}_{dtm} \cdot \boldsymbol{\gamma} + \omega_d + \delta_t + b_m,$$

where P_{dtm} is the population for the d -th day, t -th year, and m -th municipality; β_0 is the global intercept, representing the baseline log mortality rate; $\mathbf{X}_{dtm} \cdot \boldsymbol{\beta}_m$ is a non-linear function of the average daily temperature across lags 0-3 represented by a matrix of basis functions, \mathbf{X}_{dtm} , and its coefficients, $\boldsymbol{\beta}_m$, which are the combination of fixed effects $\boldsymbol{\beta}$ and random effects $\boldsymbol{\beta}_m$ of the temperature on mortality, (i.e., $\boldsymbol{\beta}_m = \boldsymbol{\beta} + \boldsymbol{\beta}_m$); \mathbf{Z}_{dtm} is a matrix representation of a set of categorical spatiotemporal confounders (the day of week and whether or not it is a public holiday), with coefficients $\boldsymbol{\gamma} = [\gamma_1, \gamma_2, \dots, \gamma_7]^T$, where γ_i ($i = 1, 2, \dots, 6$) are coefficients for the categorical variable *day of week* with Monday as the reference level and γ_7 is the coefficient for the binary variable *holiday* with non-holiday as the reference level. The final three terms ω_d , δ_t , and b_m are random effects accounting for unmeasured confounding at the level of day (i.e., to model seasonality), year (i.e., to model long-term trends), and space (i.e. to model dependency across municipalities), respectively.

To account for the non-linear relationship between temperature and mortality, we use the natural cubic splines, commonly employed in the literature for studying the temperature-mortality association (Gasparrini et al., 2015, 2022; Madaniyazi et al., 2023). Firstly, we select three knots at the 10-, 75- and, 90-th quantiles of the temperature range D and obtain the initial basis matrix \mathbf{X}'_{dtm} . Then, we select the temperature corresponding to the minimum mortality risk as the reference, which is equal to 12°C for our dataset. Lastly, to ensure that the log-relative risk is equal to 0 at the reference temperature, we rescale the initial basis matrix to be centered at 12°C by subtracting the values of each

of the four basis functions in matrix \mathbf{X}'_{dtm} at the $12^\circ C$:

$$\mathbf{X}_{dtm} = \mathbf{X}'_{dtm} - \mathbf{1} \cdot \mathbf{X}'_{[x=12]},$$

where $\mathbf{X}'_{[x=12]}$ is a four element vector containing the values of the basis matrix \mathbf{X}'_{dtm} at $12^\circ C$.

3.1.1 Prior specification

As we implement the model in a Bayesian paradigm, we specify priors for all parameters. We set a $\beta_0 \sim N(0, \infty)$ prior for the intercept and $\beta, \gamma \sim N(0, 1000)$ prior for the fixed effect parameters. As we wish for the coefficients of the basis function to vary in space, we consider a Besag, York, and Mollie (BYM2) model, which is a transformed combination of a zero-mean Gaussian prior and a intrinsic conditional autoregressive (ICAR) prior (Besag et al., 1991). Based on our specification of the basis function, let $\beta' = [\beta'_{1}, \beta'_{2}, \beta'_{3}, \beta'_{4}]$, specifically, and:

$$\beta'_{j} = \sigma_{\beta_j} \left(\sqrt{1 - \phi_{\beta_j}} \mathbf{v}_{j\star} + \sqrt{\phi_{\beta_j}} \mathbf{u}_{j\star} \right), \quad j = 1, 2, 3, 4$$

where $\mathbf{v}_{j\star}$ and $\mathbf{u}_{j\star}$ are standardised versions of two Gaussian priors \mathbf{v}_j and \mathbf{u}_j (ICAR) to have variance equal to 1 (Riebler et al., 2016). The adjacent matrix for $\mathbf{u}_{j\star}$ was defined using the queen criterion of contiguity, hence areas are neighbours if they share a common edge or a common vertex. The hyperparameter ϕ_{β_j} , known as the spatial mixing parameter, measures the proportion of marginal variance that can be explained by the structured spatial effect, \mathbf{u}_{\star} , (Besag et al., 1991). The hyperparameter σ_{β_j} is the standard deviation of the spatial field. For the residual confounding in space (b_m), we use a BYM2 prior with the hyperparameters σ_b and ϕ_b .

To account for seasonality we define a random walk 2 (RW2) process:

$$\omega_d | \omega_{d-1}, \omega_{d-2}, \sigma_\omega^2 \sim N(2\omega_{d-1} - \omega_{d-2}, \sigma_\omega^2)$$

where σ_ω^2 is the variance of the process and $\omega_{d-1}, \omega_{d-2}$ the random effect for the two days before d . For the residual confounding due to the long-term trend, we specify a zero-mean Gaussian process, $\delta_t \stackrel{\text{iid}}{\sim} N(0, \sigma_\delta^2)$, with σ_δ as the standard deviation.

3.1.2 Hyperpriors

On all the hyperparameters we specify Penalised Complexity (PC) priors. PC priors penalise model complexity according to the distance between the base (simpler) model and an alternative (more complex) model (Rue et al., 2009; Gómez Rubio, 2020; Moraga, 2019). For the standard deviation of the random effects across year, region, and spatial

varying splines we assume that the probability of it being larger than 1 (associated with mortality risks larger than $\exp(2)$) is very small (set to 0.01). We let the probability that the standard deviation of random effect across day of year is larger than 0.01 equal to 0.01. This constraint is imposed to enforce smoothness in the seasonality term while ensuring that the seasonality is accounted for within the temperature effect. For the mixing parameters, we set $Pr(\phi_{\beta_j} < 0.5) = 0.5$ and $Pr(\phi_b < 0.5) = 0.5$, reflecting our lack of knowledge about whether overdispersion or strong spatial autocorrelation should dominate the fields β and \mathbf{b} .

The model is implemented using Integrated Nested Laplace Approximation (INLA) in the R package (R-INLA) to ensure a manageable running time (R Core Team, 2024; Rue et al., 2009).

3.2 Relative mortality risk of temperature

Firstly, for computational efficiency, we define a set of values (vector \mathbf{x}) on the temperature domain D , starting from -6.81 to 29.48°C , with 200 steps (sampled from the whole temperature exposure data), $\mathbf{x} = [-6.81, 2.44, \dots, 29.48]$, derive the corresponding sampled basis matrix \mathbf{X}_s and calculate the log relative risk (RR) of temperature-related mortality in each municipality m , after accounting for confounding, as follows:

$$\begin{aligned}\log \text{RR}_m(x) &= \mathbf{X}_s \cdot \beta_m, \quad x \in \mathbf{x} \\ \beta_m &= \beta + \beta \mathbf{r}_m,\end{aligned}$$

where β is the average effect of the coefficients of the basis function across areas, and $\beta \mathbf{r}_m$ are the zero-mean spatial deviations.

The relative risk can be shown in coarser spatial resolutions that might be of public health relevance, whilst maintaining the full uncertainty. For instance, as cantons in Switzerland are responsible for their populations' healthcare and welfare, reporting results at this level could highlight differences due to different policies, preparedness, and resilience to the effect of heat. We define the posterior RR of the c -th canton ($c = 1, \dots, 26$) on the set of sampled temperature values $x \in \mathbf{x}$ as:

$$\begin{aligned}RR_c(x) &= \exp(\mathbf{X}_s \cdot \beta_c) \\ \beta_{jc} &= \sum_k \beta_{jk} \frac{P_k}{P_c}, \quad j = 1, 2, 3, 4, \quad k \in M_c\end{aligned}$$

with M_c denoting the set of municipalities that belong to the c -th canton, P_k representing the population in municipality k belonging to canton c , and P_c is the population of canton c . That is, $P_c = \sum_k P_k$, where $k \in M_c$. In this way, we retrieve the population weighted

coefficients of the basis function, that can be used to estimate the temperature-mortality curve in every canton.

3.3 Epidemiological metrics

Minimum mortality temperature (MMT): MMT is defined as the temperature with the minimum risk of death across the temperature range (Tobias et al., 2021). We estimate the municipality specific MMT based on two assumptions: the mortality risk should increase monotonically when the temperature is higher than the reference temperature ($12^\circ C$), and that the posterior probability of the RR being greater than 1 (exceedance probability) is higher than a probability threshold. To provide convincing results and account for the uncertainty of posterior results, we consider the 0.8 probability threshold.

Excess mortality rates attributable to heat (ERH): The ERH metric can be derived from the attributable fraction (AF) metric, which measures the proportion of death attributable to heat exposure among a specific population. We focus on the temperatures higher than $12^\circ C$, the reference temperature, to estimate the ERH. Following similar notation in relative mortality risk estimate in Section 3.2, we define the AF associated with heat exposure $x \in \mathbf{x}$, when $x > 12^\circ C$, and then the AF associated with a specific area m :

$$\begin{aligned} \text{AF}_m(x) &= \frac{\text{RR}_m(x) - 1}{\text{RR}_m(x)}, \quad x \in \mathbf{x}, \quad x > 12^\circ C \\ \text{AF}_m &\approx \frac{\sum w_i \Delta Y_m(x_i) h_m(x_i)}{Y_m}, \quad \text{with} \\ h_m(x_i) &= \frac{\text{AF}_m(x_{i+1}) + \text{AF}_m(x_i)}{2} \quad \text{and} \quad w_i = x_{i+1} - x_i. \\ \text{ERH}_m &= \frac{Y_m'}{P_m} = \frac{\text{AF}_m Y_m}{P_m} \end{aligned}$$

Y_m is the number of deaths in the m -th municipality, $\Delta Y_m(x_i)$ is the number of deaths in the m -th municipality occurring when the temperature varied from x_i to x_{i+1} , and $h_m(x_i)$ is the mid point of the AF values at temperatures x_i and x_{i+1} of the m -th municipality, reflecting the average value of AF in this temperature interval. Finally, we calculate the ERH by first estimating the number of deaths attributable to heat (Y_m'), also called excess mortality, and then dividing by the population (P_m) in the m -th region.

3.4 Spatial effect modifiers

To quantify the effect of the selected effect modifiers on heat-exposure spatial vulnerabilities, we use the ERH metric derived from Section 3.3 as the main outcome in the following model, where c_m is the canton which municipality m belongs to. The model for ERH is

written,

$$\begin{aligned} \text{ERH}_m &\sim \text{Normal}(\mu_m, \sigma_{\text{ERH}}^2) \\ \mu_m &= \alpha_0 + \mathbf{H}_m \cdot \boldsymbol{\alpha} + \zeta_{c_m} + \xi_m, \end{aligned}$$

where α_0 is the baseline excess mortality rate, with prior $\alpha_0 \sim N(0, \infty)$; $\boldsymbol{\alpha}$ is a vector of the coefficients of the spatial effect modifiers associated with \mathbf{H}_m , the vector of the effect modifiers at area m , and $\alpha \sim N(0, 1000)$; ζ_{c_m} captures the spatial residuals across cantons, with $\zeta_{c_m} \stackrel{\text{iid}}{\sim} N(0, \sigma_\zeta^2)$, $P(\sigma_\zeta > 1) = 0.01$; and ξ_m captures the spatial residuals across municipalities using a BYM2 prior as defined in the main model.

We show median and 95% credible intervals (CrIs) of $\boldsymbol{\alpha}$ using two approaches. In the first approach, we do not propagate the uncertainty of EHR, and use its median value for the regression. For the second approach, we take 200 samples of the posterior of EHR derived from Section 3.3, fit the above model 200 times, and summarise the posterior distributions of $\boldsymbol{\alpha}$ across the 200 samples.

3.5 Sensitivity analysis

To test the robustness of the model, the reference temperature is changed to 10°C , 15°C and 20.7°C (80th percentile of the temperature range) by centering the basis matrix of mean temperature at each of those values and rerunning the models. Letting the probability that the standard deviation of random effect across day of year is larger than 1 equal to 0.01, we also rerun the model with a less restricted prior on day of year, with the reference temperature 12°C , which is the same as that in the main analysis.

4 Results

4.1 Exploratory data analysis

The distributions of temperature and mortality among people older than 65 years is showed in Figure 1 across the summer months during 2011-2022 in Switzerland. There is an increasing trend in the mean daily temperature in the study period (panel A). For people over 65 years old, the mortality rate (panel C) decreases over the years, with a spike after 2020, which can be explained by the COVID-19 pandemic (Mathieu et al., 2020). Some seasonality patterns exist in both temperature and mortality rate time series plots. Looking at the spatial variability of temperature (panel B), we see that the average temperature in north-west part of Switzerland is higher than that in south, central or east

areas, reflecting the mountain regions, while for mortality rate (panel D), there is not a distinct spatial pattern.

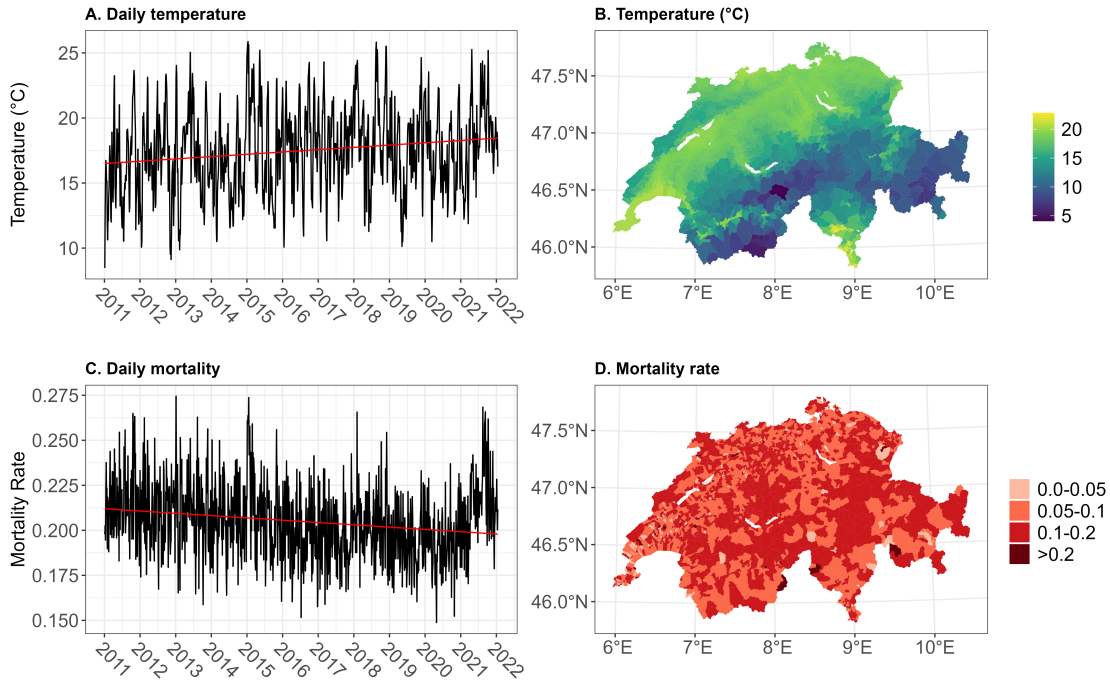


Figure 1: **A.** Daily mean temperature during summers from 2011 to 2022; **B.** Spatial pattern of the mean temperature exposure across Swiss municipalities; **C.** Daily mortality rate among people over 65 years old during summers from 2011 to 2022; **D.** Spatial pattern of the mortality rate among people over 65 years old across Swiss municipalities.

4.2 Municipality-level relative mortality risk of temperature

Panel A of Figure 2 shows the median and 95% CrIs of the overall (J-shape) effect of temperature on the relative mortality risk nationwide in Switzerland. There is weak evidence to support a temperature effect on all-cause mortality for temperatures lower than 15°C. In contrast, there is a steep increase in the mortality risk for temperatures higher than 20°C. Panel B of Figure 2 shows the median relative risk of temperature on mortality in each municipality, reflecting the variation of temperature effects at fine spatial scale. It is evident that for high temperatures, the spatial variation of the relative risk exceeds the uncertainty bands of the nationwide one.

4.3 Minimum mortality temperature (MMT)

Panel C of Figure 2 shows the distribution of MMT in each municipality across Switzerland using the 0.8 exceedance probability threshold. At the 80% probability level, only 11 areas have missing MMT values, implying there is no minimum mortality threshold temperature for the 11 areas. The overall mean MMT across Switzerland is 20.4°C at 80% level. The MMT values are relatively lower in the south part of Switzerland. In comparison, the threshold temperatures are higher in north, west and central areas.

4.4 Excess mortality rates attributable to heat (ERH)

Across the country, the overall excess deaths attributable to summer heat exposure is 2,336 (95% CrI:1,794 to 2,895) across 12 years, with an average of nearly 195 excess death counts each year in Switzerland. Panel D of Figure 2 shows that the excess mortality rate is higher in the north-west of Switzerland, with values reaching more than 2 per thousand population in some municipalities. Panel E of Figure 2 shows the exceedance probability that ERH is greater than the mean ERH across the country, and the strongest evidence corresponds to the places characterised by the highest ERH values.

Furthermore, we present the spatial distribution of attributable fraction (AF) metric, the proportion of deaths attributed to exposure to heat, in Supplementary Figure 2. In most municipalities, the median AF is less than 1%. While higher AF values are observed in the northern and western parts Switzerland, where they reached $> 10\%$ of total summer deaths in some municipalities. Additionally, Supplementary Figure 2 presents higher AF values (panel A) and stronger evidence (panel B) in some urban areas, such as Zurich, Basel and Geneva.

4.5 Aggregated cantonal-level results

The estimated cantonal-level relative mortality risk associated with temperature exposure are presented in Figure 3, while the cantonal-level J-shape relationships are shown in Supplementary Figure 3. Panel A of Figure 3 shows that Geneva is the canton where the mortality risk increases most steeply when the temperature is higher than 12°C . We also observe higher risk in Vaud, Fribourg, Graubunden, and Valais, mostly reflecting cantons in the French speaking part of Switzerland. In contrast, Appenzell Innerrhoden has the lowest risk of death due to heat exposure. Panel B of Figure 3 shows the posterior probability of the relative risk being higher than the overall mean relative risk across all cantons, capturing the uncertainty of the estimates. We report strong evidence to support that the canton of Geneva is the canton affected the most by heat exposure.

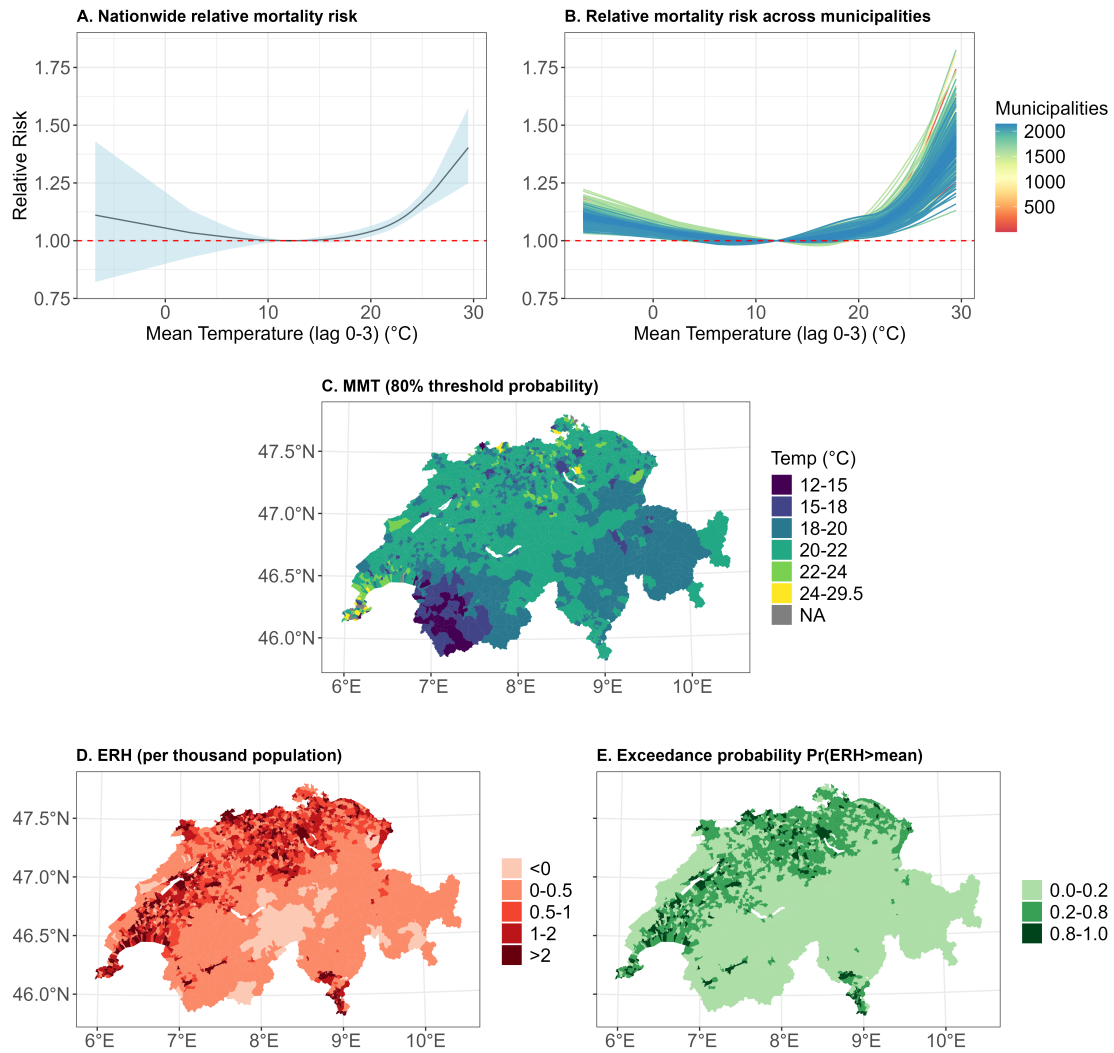


Figure 2: **A.** Nationwide temperature effect on mortality in Switzerland (the black curve represents the median estimate of the mortality relative risk (RR) compared to the risk at 12°C , and the blue shaded area represents the 95% CrI (credible interval) of the RR); **B.** Spaghetti plot of the temperature-related median mortality risk, relative to the risk at 12°C , in each municipality; **C.** Minimum mortality temperature (MMT) at 80% threshold probability, 11 missing values; **D.** Excess mortality rates attributable to heat (ERH) per thousand population ($> 12^{\circ}\text{C}$) in each municipality; **E.** The exceedance probability of ERH in the area is higher than the mean value of the ERH (1.0) across the country.

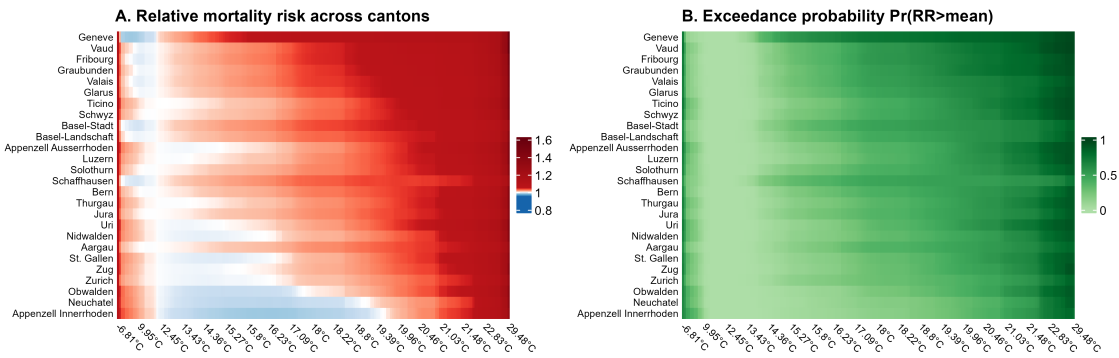


Figure 3: **A.** The median value of mortality relative risk (RR), compared to the risk at 12°C , in each canton; **B.** The exceedance probability of RR is higher than the mean value (1.04) across the country in each canton.

4.6 Spatial effect modifiers

Panel A of Figure 4 shows the effect of spatial effect modifiers on the ERH, with and without uncertainty propagation. After propagating the uncertainty, one standard deviation increase in the proportion of people older than 85 years (3.16%) corresponds to 0.30 (95% CrI: 0.18 to 0.47) more deaths per 1,000 people due to heat exposure. Access to green space was also found to affect the observed health related vulnerabilities to heat exposure. One standard deviation increase in green space coverage (0.12 of the NDVI) is associated with 0.57 (95% CrI: 0.35 to 0.77) less deaths per 1,000 people due to heat exposure. Areas with higher average temperature exposure are characterised with higher excess mortality rate, with one standard deviation (2.67°C) increase in the average temperature leading to 1.08 (95% CrI: 0.79 to 1.38) more deaths per 1,000 people due to acute heat exposure. The distributions of the continuous effect modifiers and their respective standard deviations are shown in panel B of Figure 4. There is weak evidence of an association between the other covariates and excess mortality rate attributable to heat exposure. The results of the model without uncertainty propagation are consistent, but, as expected, the CrIs are narrower (panel A of Figure 4).

4.7 Sensitivity analysis

The model framework provides stable results with different reference temperature values, see Supplementary Figure 4. Comparing with our main results in Figure 2, after changing the prior on day of year to the less restricted one, we observe similar results, see Supplementary Figure 5.

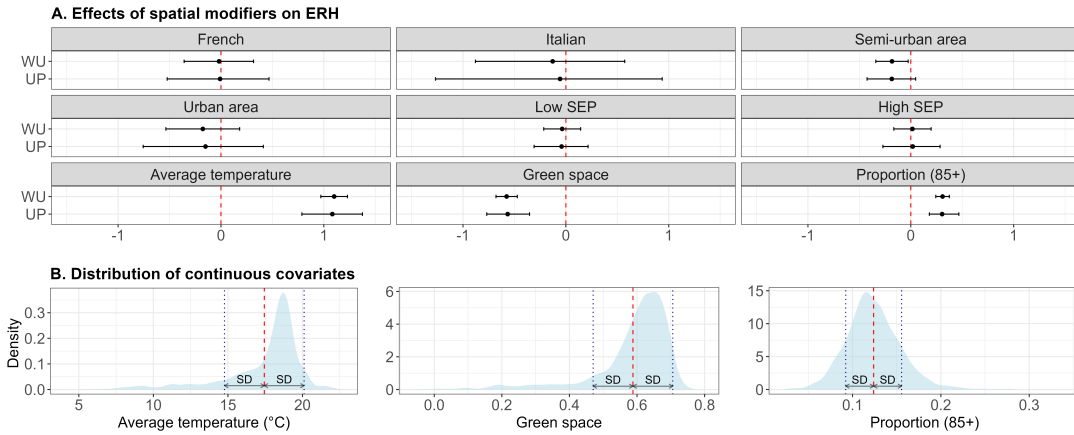


Figure 4: **A.** The effects of covariates on heat-related excess mortality rate (ERH) using without uncertainty (WU) and uncertainty propagation (UP) approaches; **B.** The distribution of continuous spatial effect modifiers (the shaded blue areas represent the probability density distributions of the variables, the red dashed lines show the mean of each variable, and the dark blue dotted lines show the standard deviation (SD) of each variable).

5 Discussion

This study introduces a flexible modelling framework to account for the spatial variation in the non-linear relationships between heat and mortality across small spatial units. By leveraging the posterior distribution of the model parameters, the approach derives key epidemiological metrics, including excess mortality attributable to heat exposure and minimum mortality temperature, to comprehensively assess the health impacts of heat. Set within a Bayesian framework, the approach fully propagates the uncertainty associated with model parameters into the derived epidemiological metrics and obtains aggregated estimates at any administrative level, such as cantons, deemed particularly relevant for policymakers. Lastly, we extend our analysis by incorporating a second-stage model to investigate the role of environmental and social effect modifiers in shaping spatial patterns of vulnerability.

5.1 Comparison with previous epidemiological studies

Our results are consistent with previous epidemiological studies focusing on estimating the temperature-mortality relationships (Gasparrini et al., 2015; Wicki et al., 2024; Masselot et al., 2023). We report approximately 195 deaths in people older than 65 years per summer in Switzerland. This is lower but compatible with the 95% CrI with a previous study focusing on excess mortality during the summer 2022 in Switzerland (Konstanti-

noudis et al., 2023a). The observed J-shape relationship is consistent with the previous studies in Japan, USA, Italy and Australia (Gasparrini et al., 2015), and Switzerland (Vicedo-Cabrera et al., 2023). A nationwide study in Switzerland during summers from 2003 to 2016 shows a 20°C threshold for mean temperature, which is consistent with our MMT estimate (Ragettli et al., 2023). However, in line with a previous study in England and Wales, we observed significant spatial variation of the MMT distribution across small areas (Gasparrini et al., 2022).

Previous studies have reported spatial vulnerabilities in heat exposure across small areas (Konstantinoudis et al., 2022; Bennett et al., 2014; Gasparrini et al., 2022). Studies in England and Wales found higher vulnerability of heat-related mortality in urban areas and older populations (Gasparrini et al., 2022; Bennett et al., 2014). In contrast, another study in England focusing on chronic obstructive pulmonary disease hospital admissions reported weak evidence of a protective effect of green space and average temperature (Konstantinoudis et al., 2022). In line with the previous studies, we also report higher vulnerabilities in older populations and evidence of a protective effect of green space. This can be explained by the impaired mechanisms of older populations to regulate heat, and also by the fact that green spaces modify heat exposure (Arsad et al., 2022; Markevych et al., 2017). However, we observed that average temperature increases heat-related vulnerabilities. Higher averaged temperature can be a proxy for higher air pollution exposure which could directly or indirectly, by aggravating chronic diseases, can increase vulnerability to heat (Zhang et al., 2024).

5.2 Comparison with previous models

Previous studies leveraging data from multiple countries and cities worldwide, with no explicit spatial structure that needs to be incorporated, have employed a time-series approach that accounts for lags and non-linear temperature effects (Gasparrini et al., 2010; Vicedo-Cabrera et al., 2023; Gasparrini et al., 2015; Masselot et al., 2023; Gasparrini et al., 2012). These analyses are typically conducted independently at the first stage, with the resulting estimates pooled using meta-regression. This methodology has been also applied to nationwide and multi-county studies using smaller areas with prominent spatial structures (Gasparrini et al., 2022; Vicedo-Cabrera et al., 2023; Ballester et al., 2023). When the main unit of analysis is small areas, the above approach encounters two interconnected challenges: data sparsity at the small-area level and the lack of a component that captures spatial dependencies. Sparse data can lead to unstable estimates, characterised by high variability, while not accounting for spatial correlation brings vari-

ance underestimation (Koldasbayeva et al., 2024). Using spatial priors that incorporate spatial structures can smooth estimates, providing more stable and reliable results in the presence of sparse data (Gasparrini and Ben, 2013; Konstantinoudis et al., 2019).

Previous studies have also developed linear threshold models to capture the J-shaped relationship between heat exposure and mortality (Konstantinoudis et al., 2022; Bennett et al., 2014). These models incorporate spatial priors to account for spatial dependencies in the slope above the threshold (Konstantinoudis et al., 2022; Bennett et al., 2014). While the results are easy to communicate and interpret, these models face challenges in identifying thresholds, and two linear segments are might not fully capture the non-linear effect of temperature on health.

A recent study in Barcelona proposed a spatial Bayesian distributed lag non-linear model framework that accounts for the spatial dependencies of the non-linear temperature-mortality relationship in 73 neighborhoods in Barcelona (Quijal-Zamorano et al., 2024). This model provides a first step in disentangling the non-linear spatial inequalities of heat exposure on health. In our approach, we extend this model in several ways. First, we introduce a population offset and a spatial random effect in the model. The population offset is crucial in small-area studies as population can confound the exposure response relationship. In case of heat exposure, small areas with higher populations, especially within large cities, can be proxies for factors that confound the temperature-mortality relationship such as buildings, green space access and air pollution. Second, we included a spatial random effect to account for remaining unobserved spatial factors that confound the heat-mortality relationship, such as deprivation. Third, we selected different priors. For the spatial random effect, we selected a BYM2 prior instead of the Leroux prior. The marginal variance of the spatial field in the Leroux prior depends on the graph structure. The BYM2 model is defined by standardising the spatial and non-spatial random effects, facilitating interpretable hyperprior assignment and hyperparameter interpretation (ensures the same interpretation in different applications) (Besag et al., 1991; Leroux et al., 2000; Sørbye and Rue, 2014). Additionally, we also used PC priors to ensure the parsimony of the model and avoid the risk of overfitting according to the distance from the simplest base model (Gómez Rubio, 2020). Fourth, we scaled the framework to fit large epidemiological datasets and examined variable aspects of the mortality-heat relationship. Focusing on Switzerland, we used 12 years worth of data, 2,145 small areas and the INLA algorithm for quick and accurate inference (Rue et al., 2009). We exploited the Bayesian framework to show different epidemiological metrics, and different policy-relevant aggregations, while fully propagating parameter uncertainty. Lastly, we also proposed a second stage model to quantify the potential sources of the observed spatial inequalities by se-

lected small-area environmental and social covariates.

Our work has some limitations. First, although we explained the spatial vulnerability with environmental and socio-demographic variables, the spatial variation of heat-related vulnerability can also be explained by other individual-level variables, such as medication and chronic conditions. Such granular information was not available. Second, while the analysis incorporated data from multiple years, the model accounts only for the spatially varying effects of temperature. The assumption of a constant heat-mortality relationship over time might not hold, as previous studies have reported adaptive mechanisms to heat over time (Konstantinou et al., 2023b). Within the proposed framework, it is straightforward to let the coefficients of the basis function to vary in time, using priors with temporal structures, such as random walks and autoregressive processes (Vicedo-Cabrera et al., 2018). However, we chose not to pursue this approach, as the primary objective of this study was to disentangle spatial inequalities. Disregarding temporal variation is unlikely to substantially impact the results while offering a computationally less intensive model. Finally, rather than including temperature exposures at individual lags to capture delayed effects, we calculated the average temperature across 0-3 time lags, as shorter lags are relevant when assessing heat exposure. However, when examining exposures with longer lags, it would be important to extend this approach to account for potential non-linear structures in the lag dimension.

In summary, in this work, we present a scalable framework to describe the spatial variation of the heat-mortality effect across small areas. The framework can be expanded to capture spatial, temporal and spatiotemporal vulnerabilities of the health-related burden of temperature exposure. Applied to Switzerland, our framework provides valuable insights for mitigation strategies and the reduction of spatial inequalities in the health impacts of heat exposure. We emphasize the significance of older populations and green space in shaping spatial vulnerabilities, as well as the marked spatial variation in the MMTs. Consequently, we suggest targeted interventions for older populations, region-specific heat warnings that incorporate varying MMTs, and a greater emphasis on green space in urban planning.

Code and data availability

R code is publicly available on GitHub <https://github.com/fxinyichen/SwissHeat>. The data set is available on https://drive.google.com/drive/folders/15FNaf4x1tkhg1BjnR0mYY6G0idEkWBWn?usp=drive_link.

Competing interests

The authors declare no competing interests.

Author contributions statement

G.K. conceived the study. G.K. and M.B. supervised the study. G.K. prepared the mortality, population and covariate data. X.C. developed the statistical model, wrote the code for the analysis and extracted the results. X.C. wrote the initial draft and all the authors contributed in modifying the paper and critically interpreting the results. All authors read and approved the final version for publication.

Acknowledgments

G.K. is supported by an Imperial College Research Fellowship.

References

- Arsad, F., Hod, R., Ahmad, N., Ismail, R., Mohamed, N., Baharom, M., Osman, Y., Radi, M., and Tangang, F. (2022). The impact of heatwaves on mortality and morbidity and the associated vulnerability factors: A systematic review. *International Journal of Environmental Research and Public Health*, 19:16356. <https://doi.org/10.3390/ijerph192316356>.
- Baccini, M., Biggeri, A., Accetta, G., Kosatsky, T., Katsouyanni, K., Analitis, A., Anderson, H., Bisanti, L., D'Ippoliti, D., Danova, J., Forsberg, B., Medina, S., Paldy, A., Rabczenko, D., Schindler, C., and Michelozzi, P. (2008). Heat effects on mortality in 15 european cities. *Epidemiology (Cambridge, Mass.)*, 19:711–719. <https://doi.org/10.1097/EDE.0b013e318176bfcd>.
- Ballester, J., Quijal-Zamorano, M., Turrubiates, R., Pegenaute, F., Herrmann, F., Robine, J.-M., Basagaña, X., Tonne, C., Antó, J., and Achebak, H. (2023). Heat-related mortality in europe during the summer of 2022. *Nature Medicine*, 29:1–10. <https://doi.org/10.1038/s41591-023-02419-z>.
- Bennett, J. E., Blangiardo, M., Fecht, D., Elliott, P., and Ezzati, M. (2014). Vulnerability to the mortality effects of warm temperature in the districts of England and

- Wales. *Nature Climate Change*, 4(4):269–273. https://ideas.repec.org/a/nat/natcli/v4y2014i4d10.1038_nclimate2123.html.
- Besag, J., York, J., and Mollié, A. (1991). Bayesian image restoration, with two applications in spatial statistics. *Annals of the Institute of Statistical Mathematics*, 71:1–59. <https://doi.org/10.1007/BF00116466>.
- de Schrijver, E., Folly, C. L., Schneider, R., Royé, D., Franco, O. H., Gasparrini, A., and Vicedo-Cabrera, A. M. (2021). A comparative analysis of the temperature-mortality risks using different weather datasets across heterogeneous regions. *Geo-Health*, 5(5):e2020GH000363.
- Ebi, K. L., Capon, A., Berry, P., Broderick, C., de Dear, R., Havenith, G., Honda, Y., Kovats, R. S., Ma, W., Malik, A., Morris, N. B., Nybo, L., Seneviratne, S. I., Vanos, J., and Jay, O. (2021). Hot weather and heat extremes: health risks. *The Lancet*, 398(10301):698–708. <https://www.sciencedirect.com/science/article/pii/S0140673621012083>.
- eurostat (2011). *Degree of urbanisation classification*. https://ec.europa.eu/eurostat/statistics-explained/index.php?title=Degree_of_urbanisation_classification_-_2011_revision [Accessed 23rd October 2024].
- Federal Statistical Office (2010). *Spatial divisions*. <https://www.bfs.admin.ch/bfs/de/home/statistiken/querschnittsthemen/raeumliche-analysen/raeumliche-gliederungen.html> [Accessed 23rd October 2024].
- Federal Statistical Office (2024). *Population*. <https://www.bfs.admin.ch/bfs/en/home/statistics/population.html> [Accessed 14th February 2024].
- Gasparrini, A. (2022). A tutorial on the case time series design for small-area analysis. *BMC Medical Research Methodology*, 22. <https://api.semanticscholar.org/CorpusID:248498944>.
- Gasparrini, A. and Armstrong, B. (2010). Time series analysis on the health effects of temperature: Advancements and limitations. *Environmental research*, 110:633–8. <https://doi.org/10.1016/j.envres.2010.06.005>.
- Gasparrini, A., Armstrong, B., and Kenward, M. G. (2010). Distributed lag non-linear models. *Statistics in Medicine*, 29(21):2224–2234. <https://onlinelibrary.wiley.com/doi/abs/10.1002/sim.3940>.

- Gasparrini, A., Armstrong, B., and Kenward, M. G. (2012). Multivariate meta-analysis for non-linear and other multi-parameter associations. *Statistics in Medicine*, 31(29):3821–3839. <https://onlinelibrary.wiley.com/doi/abs/10.1002/sim.5471>.
- Gasparrini, A. and Ben, A. (2013). Reducing and meta-analysing estimates from distributed lag non-linear models. *BMC Medical Research Methodology*, 13(1).
- Gasparrini, A., Guo, Y., Hashizume, M., Lavigne, E., Zanobetti, A., and Schwartz, J. (2015). Mortality risk attributable to high and low ambient temperature: a multicountry observational study. *Lancet*, 386. [https://doi.org/10.1016/S0140-6736\(14\)62114-0](https://doi.org/10.1016/S0140-6736(14)62114-0).
- Gasparrini, A., Masselot, P., Scortichini, M., Schneider, R., Mistry, M. N., Sera, F., Macintyre, H. L., Phalkey, R., and Vicedo-Cabrera, A. M. (2022). Small-area assessment of temperature-related mortality risks in england and wales: a case time series analysis. *The Lancet Planetary Health*, 6(7):e557–e564. <https://www.sciencedirect.com/science/article/pii/S2542519622001383>.
- Gómez Rubio, V. (2020). *Bayesian Inference with INLA*. Chapman and Hall/CRC. <https://doi.org/10.1201/9781315175584>.
- Koldasbayeva, D., Tregubova, P., Gasanov, M., Zaytsev, A., Petrovskaia, A., and Burnaev, E. (2024). Challenges in data-driven geospatial modeling for environmental research and practice. *Nature Communications*, 15.
- Konstantinoudis, G., Hauser, A., and Riou, J. (2023a). Bayesian ensemble modelling to monitor excess deaths during summer 2022 in switzerland. *arXiv preprint arXiv:2308.15251*.
- Konstantinoudis, G., Minelli, C., Lam, H. C. Y., Fuertes, E., Ballester, J., Davies, B., Vicedo-Cabrera, A. M., Gasparrini, A., and Blangiardo, M. (2023b). Asthma hospitalisations and heat exposure in england: a case–crossover study during 2002–2019. *Thorax*, 78(9):875–881.
- Konstantinoudis, G., Minelli, C., Vicedo-Cabrera, A. M., Ballester, J., Gasparrini, A., and Blangiardo, M. (2022). Ambient heat exposure and copd hospitalisations in england: a nationwide case-crossover study during 2007-2018. *Thorax*, 77(11):1098—1104. <https://europepmc.org/articles/PMC9606528>.
- Konstantinoudis, G., Schuhmacher, D., Ammann, R., Diesch-Furlanetto, T., Kuehni, C., and Spycher, B. (2019). Bayesian spatial modelling of childhood cancer incidence in

- switzerland using exact point data: A nationwide study during 1985-2015. *International Journal of Health Geographics*.
- Leroux, B., Lei, X., and Breslow, N. (2000). Estimation of disease rates in small areas: A new mixed model for spatial dependence. *Institute for Mathematics and Its Applications*, 116.
- Madaniyazi, L., Tobías, A., Vicedo-Cabrera, A. M., Jaakkola, J. J. K., Honda, Y., Guo, Y., Schwartz, J., Zanobetti, A., Bell, M. L., Armstrong, B., Campbell, M. J., Katsouyanni, K., Haines, A., Ebi, K. L., Gasparri, A., and Hashizume, M. (2023). Should we adjust for season in time-series studies of the short-term association between temperature and mortality? *Epidemiology (Cambridge, Mass.)*, 34(3):313–318. <https://doi.org/10.1097/ede.0000000000001592>.
- Markevych, I., Schoierer, J., Hartig, T., Chudnovsky, A., Hystad, P., Dzhambov, A., de Vries, S., Triguero-Mas, M., Brauer, M., Nieuwenhuijsen, M., Lupp, G., Richardson, E., Astell-Burt, T., Dimitrova, D., Feng, X., Sadeh, M., Standl, M., and Fuentes, E. (2017). Exploring pathways linking greenspace to health: Theoretical and methodological guidance. *Environmental Research*, 158:301–317. <https://doi.org/10.1016/j.envres.2017.06.028>.
- Masselot, P., Mistry, M., Vanoli, J., Schneider, R., Iungman, T., Garcia-Leon, D., Ciscar, J.-C., Feyen, L., Orru, H., Urban, A., Breitner, S., Huber, V., Schneider, A., Samoli, E., Stafoggia, M., de’Donato, F., Rao, S., Armstrong, B., Nieuwenhuijsen, M., Vicedo-Cabrera, A. M., Gasparri, A., MCC Collaborative Research Network, and EXHAUSTION project (2023). Excess mortality attributed to heat and cold: a health impact assessment study in 854 cities in europe. *The Lancet. Planetary health*, 7(4):e271–e281. http://repositori.upf.edu/bitstream/10230/57139/1/Masselot_lph_exce.pdf.
- Mathieu, E., Ritchie, H., Rodés-Guirao, L., Appel, C., Giattino, C., Hasell, J., Macdonald, B., Dattani, S., Beltekian, D., Ortiz-Ospina, E., and Roser, M. (2020). Coronavirus pandemic (covid-19). *Our World in Data*. <https://ourworldindata.org/coronavirus>.
- MeteoSwiss (2020). *Spatial Climate analysis*. <https://www.meteoswiss.admin.ch/climate/the-climate-of-switzerland/spatial-climate-analyses.html> [Accessed 14th February 2024].
- Moraga, P. (2019). *Geospatial Health Data: Modeling and Visualization with R-INLA and Shiny*. Chapman & Hall/CRC Biostatistics Series. <https://www.paulamoraga.com/book-geospatial/index.html>.

- Nager.Date (2024). *Worldwide public holiday*. <https://date.nager.at/> [Accessed 19th June 2024].
- Panczak, R., Galobardes, B., Voorpostel, M., Spoerri, A., Zwahlen, M., and Egger, M. (2012). A swiss neighbourhood index of socioeconomic position: Development and association with mortality. *Journal of epidemiology and community health*, 66. <https://doi.org/10.1136/jech-2011-200699>.
- Quijal-Zamorano, M., Martinez-Beneito, M. A., Ballester, J., and Mari-Dell’Olmo, M. (2024). Spatial Bayesian distributed lag non-linear models (SB-DLNM) for small-area exposure-lag-response epidemiological modelling. *International Journal of Epidemiology*, 53(3):dyae061. <https://doi.org/10.1093/ije/dyae061>.
- R Core Team (2024). *R: A Language and Environment for Statistical Computing*. R Foundation for Statistical Computing, Vienna, Austria. <https://www.R-project.org/>.
- Ragetti, M., Saucy, A., Flückiger, B., Vienneau, D., Hoogh, K. d., Vicedo-Cabrera, A., Schindler, C., and Rössli, M. (2023). Explorative assessment of the temperature–mortality association to support health-based heat-warning thresholds: A national case-crossover study in switzerland. *International Journal of Environmental Research and Public Health*, 20:4958. <https://doi.org/10.3390/ijerph20064958>.
- Riebler, A., Sørbye, S., Simpson, D., and Rue, H. (2016). An intuitive bayesian spatial model for disease mapping that accounts for scaling. *Statistical Methods in Medical Research*, 25:1145–1165.
- Rue, H., Martino, S., and Chopin, N. (2009). Approximate bayesian inference for latent gaussian models by using integrated nested laplace approximations. *Journal of the Royal Statistical Society Series B*, 71:319–392. <https://doi.org/10.1111/j.1467-9868.2008.00700.x>.
- Swiss Data Cube (2020). *Normalized Difference Vegetation Index (NDVI) - Annual Mean - Switzerland*. <https://yareta.unige.ch/archives/b6022b1c-1c59-4fc7-8a76-1b68c3c07dc7> [Accessed 23rd October 2024].
- Sørbye, S. H. and Rue, H. (2014). Scaling intrinsic gaussian markov random field priors in spatial modelling. *Spatial Statistics*, 8:39–51. Spatial Statistics Miami.
- Tobias, A., Hashizume, M., Honda, Y., Sera, F., Ng, C. F. S., Kim, Y., Royé, D., Chung, Y., Tran, N. D., Kim, H., Lee, W., Íñiguez, C., Vicedo-Cabrera, A., Abrutsky, R., Guo,

- Y., Tong, S., Coelho, M., Saldiva, P., Lavigne, E., and Carrasco-Escobar, G. (2021). Geographical variations of the minimum mortality temperature at a global scale. *Environmental Epidemiology*, 5:e169. <https://doi.org/10.1097/ee9.000000000000169>.
- Vicedo-Cabrera, A., de Schrijver, E., Schumacher, D., Ragetti, M., Fischer, E., and Seneviratne, S. (2023). The footprint of human-induced climate change on heat-related deaths in the summer of 2022 in Switzerland. *Environmental Research Letters*, 18. <https://doi.org/10.1088/1748-9326/ace0d0>.
- Vicedo-Cabrera, A. M., Sera, F., Guo, Y., Chung, Y., Arbutnott, K., Tong, S., Tobias, A., Lavigne, E., de Sousa Zanotti Stagliorio Coelho, M., Hilario Nascimento Saldiva, P., Goodman, P. G., Zeka, A., Hashizume, M., Honda, Y., Kim, H., Ragetti, M. S., Röösli, M., Zanobetti, A., Schwartz, J., Armstrong, B., and Gasparrini, A. (2018). A multi-country analysis on potential adaptive mechanisms to cold and heat in a changing climate. *Environment International*, 111:239–246.
- Wicki, B., Flückiger, B., Vienneau, D., de Hoogh, K., Röösli, M., and Ragetti, M. S. (2024). Socio-environmental modifiers of heat-related mortality in eight Swiss cities: A case time series analysis. *Environmental Research*, 246:118116. <https://www.sciencedirect.com/science/article/pii/S0013935124000203>.
- Zhang, S., Breitner, S., Stafoggia, M., de' Donato, F., Samoli, E., Zafeiratou, S., Katsouyanni, K., Rao, S., Diz-Lois Palomares, A., Gasparrini, A., Masselot, P., Nikolaou, N., Aunan, K., Peters, A., and Schneider, A. (2024). Effect modification of air pollution on the association between heat and mortality in five European countries. *Environmental Research*, 263:120023.
- Èrica Martínez-Solanas, Quijal-Zamorano, M., Achebak, H., Petrova, D., Robine, J.-M., Herrmann, F. R., Rodó, X., and Ballester, J. (2021). Projections of temperature-attributable mortality in Europe: a time series analysis of 147 contiguous regions in 16 countries. *The Lancet Planetary Health*, 5(7):e446–e454. <https://www.sciencedirect.com/science/article/pii/S2542519621001509>.

Online Supplement of 'Modelling the Spatially Varying Non-Linear Effects of Heat Exposure'

Xinyi Chen¹, Marta Blangiardo¹, Connor Gascoigne¹, and Garyfallos
Konstantinoudis^{2,*}

¹MRC Centre for Environment and Health, School of Public Health, Imperial
College London, London, UK

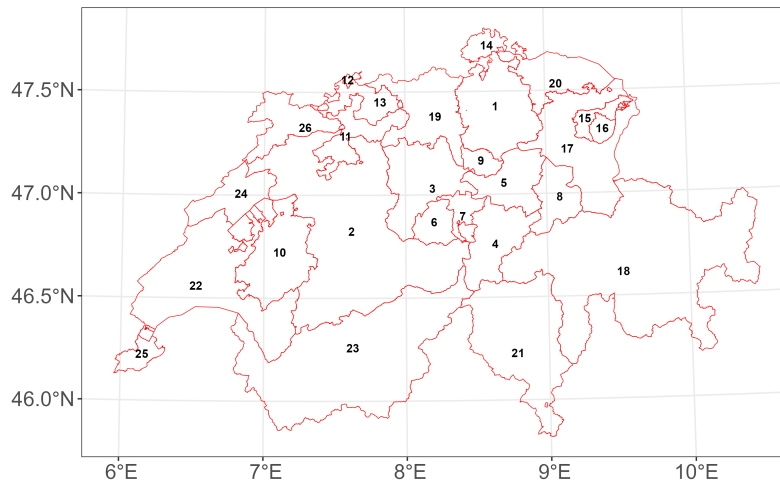
²Grantham Institute for Climate Change and the Environment, Imperial
College London, London, UK

* Corresponding author. Garyfallos Konstantinoudis, Grantham Institute for
Climate Change and the Environment, Imperial College London, London, UK.
g.konstantinoudis@imperial.ac.uk

List of Supplementary Figures

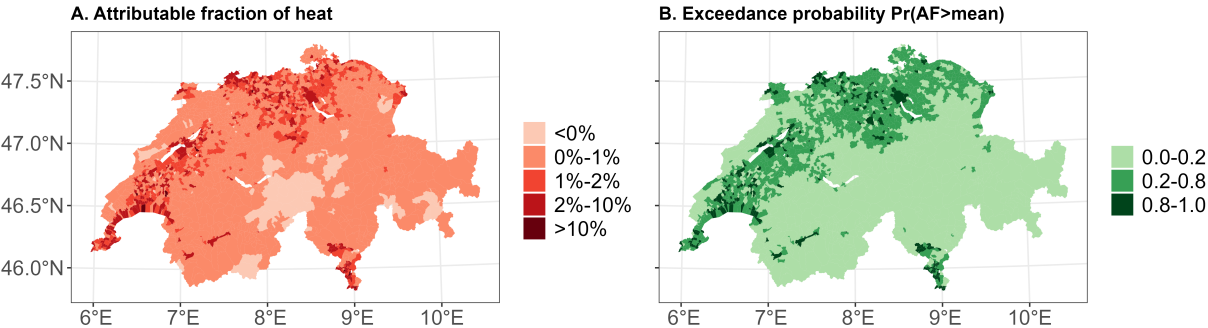
1	Map of the cantons in Switzerland.	3
2	A. Fraction of deaths attributable to heat (when temperature is higher than the reference $12^{\circ}C$) in each municipality; B. The exceedance probability of the attributable fraction (AF) in the area is higher than the mean value (0.998%) across the country.	4
3	Effects of temperature on mortality in each canton.	5
4	Spaghetti plots of median values of effect in each municipality with reference temperatures $10^{\circ}C$ (panel A), $15^{\circ}C$ (panel B) and $20.7^{\circ}C$ (panel C).	6
5	Sensitivity analysis results with less restricted prior on day of year for A. Nationwide temperature effect on mortality in Switzerland (the black curve represents the median estimate of the mortality relative risk (RR) compared to the risk at $12^{\circ}C$, and the blue shaded area represents the 95% CrI (credible interval) of the RR); B. Spaghetti plot of the temperature-related median mortality risk, relative to the risk at $12^{\circ}C$, in each municipality; C. Minimum mortality temperature (MMT) at 80% threshold probability, 12 missing values; D. Excess mortality rates attributable to heat (ERH) per thousand population ($> 12^{\circ}C$) in each municipality; E. The exceedance probability of ERH in the area is higher than the mean value of the ERH (1.0) across the country.	7

Supplementary Figure 1: Map of the cantons in Switzerland.

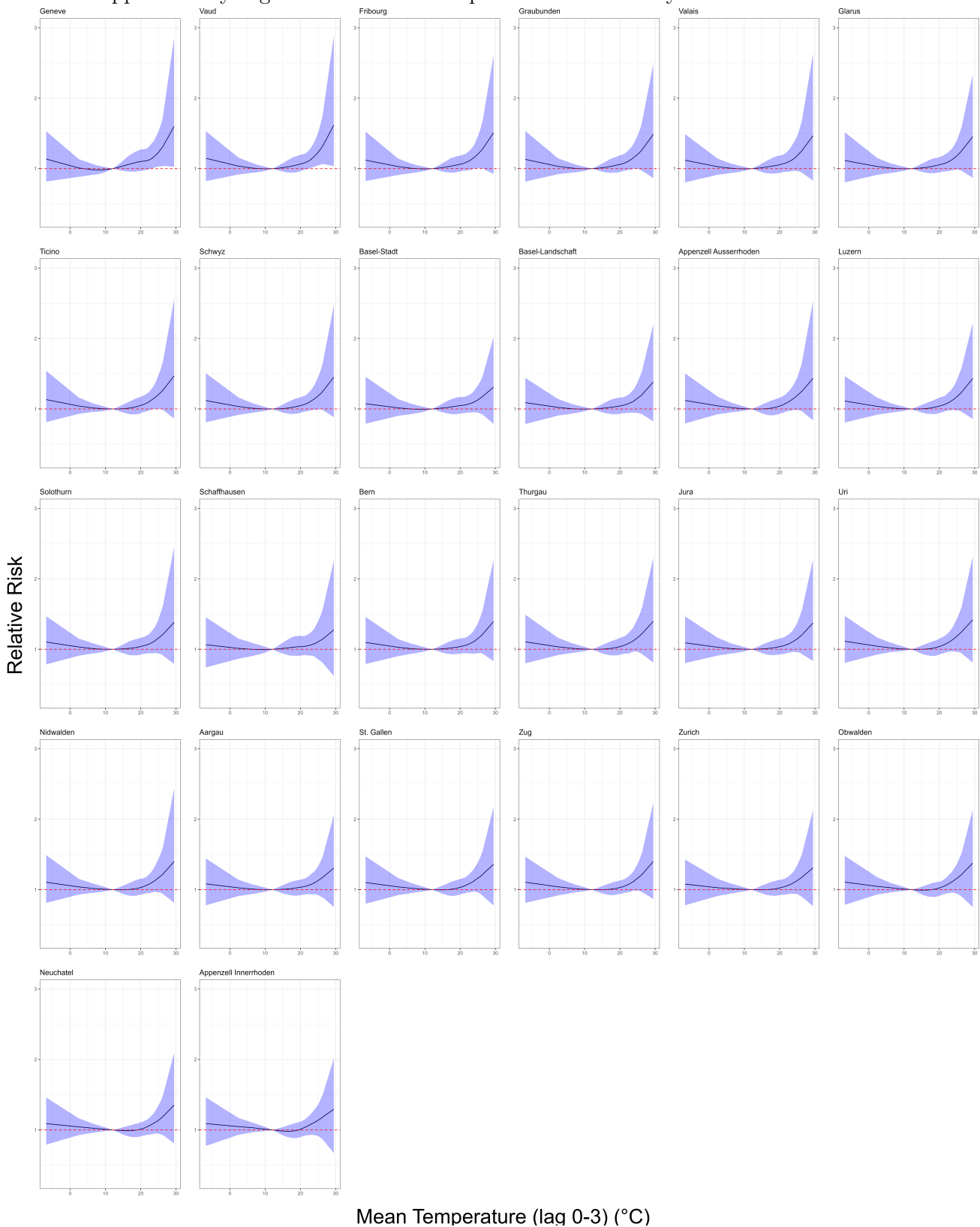


- | | |
|-----------------------|-----------------------------|
| 1 - Zurich | 14 - Schaffhausen |
| 2 - Bern | 15 - Appenzell Ausserrhoden |
| 3 - Luzern | 16 - Appenzell Innerrhoden |
| 4 - Uri | 17 - St. Gallen |
| 5 - Schwyz | 18 - Graubunden |
| 6 - Obwalden | 19 - Aargau |
| 7 - Nidwalden | 20 - Thurgau |
| 8 - Glarus | 21 - Ticino |
| 9 - Zug | 22 - Vaud |
| 10 - Fribourg | 23 - Valais |
| 11 - Solothurn | 24 - Neuchatel |
| 12 - Basel-Stadt | 25 - Geneve |
| 13 - Basel-Landschaft | 26 - Jura |

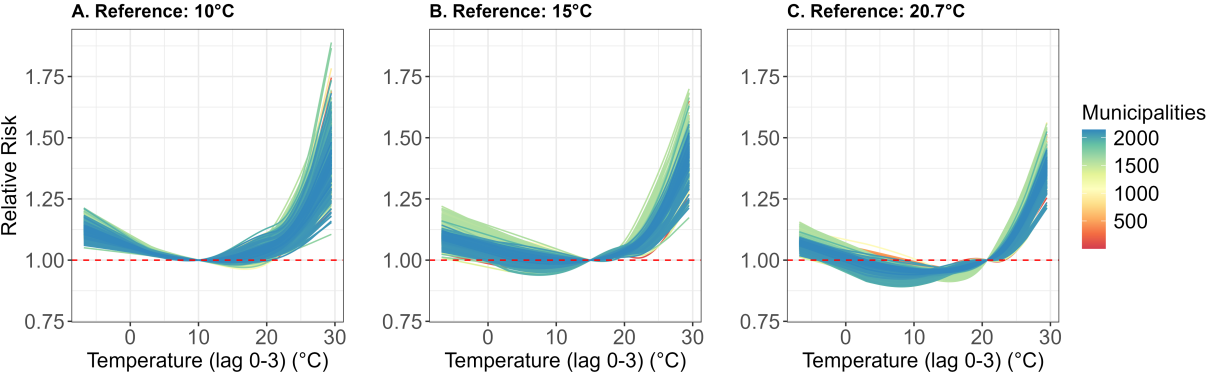
Supplementary Figure 2: **A.** Fraction of deaths attributable to heat (when temperature is higher than the reference $12^{\circ}C$) in each municipality; **B.** The exceedance probability of the attributable fraction (AF) in the area is higher than the mean value (0.998%) across the country.



Supplementary Figure 3: Effects of temperature on mortality in each canton.



Supplementary Figure 4: Spaghetti plots of median values of effect in each municipality with reference temperatures 10°C (panel **A**), 15°C (panel **B**) and 20.7°C (panel **C**).



Supplementary Figure 5: Sensitivity analysis results with less restricted prior on day of year for **A**. Nationwide temperature effect on mortality in Switzerland (the black curve represents the median estimate of the mortality relative risk (RR) compared to the risk at 12°C , and the blue shaded area represents the 95% CrI (credible interval) of the RR); **B**. Spaghetti plot of the temperature-related median mortality risk, relative to the risk at 12°C , in each municipality; **C**. Minimum mortality temperature (MMT) at 80% threshold probability, 12 missing values; **D**. Excess mortality rates attributable to heat (ERH) per thousand population ($> 12^{\circ}\text{C}$) in each municipality; **E**. The exceedance probability of ERH in the area is higher than the mean value of the ERH (1.0) across the country.

